The Surface Dependence of CO Adsorption on Ceria

ARTICLE *in* THE JOURNAL OF PHYSICAL CHEMISTRY B · SEPTEMBER 2006

Impact Factor: 3.3 · DOI: 10.1021/jp062499a · Source: PubMed

2 AUTHORS:

Michael Nolan
University College Cork
88 PUBLICATIONS **2,364** CITATIONS
SEE PROFILE

Graeme W Watson
Trinity College Dublin
203 PUBLICATIONS **6,797** CITATIONS
SEE PROFILE

The Surface Dependence of CO Adsorption on Ceria

Michael Nolan[†,‡] and Graeme W. Watson*[,†,§]

School of Chemistry, University of Dublin, Trinity College, Dublin 2, Ireland, and Trinity Centre for High Performance Computing, University of Dublin, Trinity College, Dublin 2, Ireland

Received: April 24, 2006; In Final Form: June 14, 2006

An understanding of the interaction between ceria and environmentally sensitive molecules is vital for developing its role in catalysis. We present the structure and energetics of CO adsorbed onto stoichiometric (111), (110), and (100) surfaces of ceria from first principles density functional theory corrected for on-site Coulomb interactions, DFT+U. DFT+U is applied because it can describe consistently the properties of both the stoichiometric and reduced surfaces. Our major finding is that the interaction is strongly surface dependent, consistent with experiment. Upon interaction of CO with the (111) surface, weak binding is found, with little perturbation to the surface or the molecule. For the (110) and (100) surfaces, the most stable adsorbate is that in which the CO molecule bridges two oxygen atoms and pulls these atoms out of their lattice sites, with formation of a (CO_3) species. This results in a strong modification to the surface structure, consistent with that resulting from mild reduction. The electronic structure also demonstrates reduction of the ceria surface and consequent localization of charge on cerium atoms neighboring the vacancy sites. The surface-bound (CO_3) species is identified as a carbonate, $(CO_3)^{2-}$ group, which is formed along with two reduced surface Ce(III) ions, in good agreement with experimental infrared data. These results provide a detailed investigation of the interactions involved in the adsorption of CO on ceria surfaces, allowing a rationalization of experimental findings and demonstrate further the applicability of the DFT+U approach to the study of systems in which reduced ceria surfaces play a role.

1. Introduction

Due to the relative ease with which it can be reduced (formation of oxygen vacancies) and reoxidized, ceria is of importance in catalysis.[1] This facile storage and release of oxygen for catalytic reactions is known as the oxygen storage capacity (OSC). Among the important reactions catalyzed by stoichiometric ceria is the oxidation of CO to CO_2[2] with reduction of the surface,[3] i.e., the formation of oxygen vacancies; see Figure 1. Although this reaction is important, and there exists recent experimental data that have clarified the surface sensitivity of the interaction of CO with ceria, there has been little theoretical progress toward a comprehensive understanding of the factors driving this interaction.

Early experimental data from Li et al. points to formation of a carbonate, $(CO_3)^{2-}$, species upon interaction of CO with stoichiometric ceria. The infrared (IR) vibrational spectrum showed vibrational bands characteristic of carbonate.[3] The same experiments also indicated that there also exists a weak adsorption mode, in which an intact CO molecule is oriented over a single Ce(IV) ion—the CO in this situation can be easily desorbed at temperatures above room temperature. However, in these studies, the ceria sample was a powder, and thus, no conclusions regarding surface sensitivity could be established. Later work[4,5] has provided evidence of the surface sensitivity of the CO-ceria interaction through studying ceria nanorods and nanoparticles[4] and polycrystalline ceria.[5] Ceria nanorods have been shown to expose (110) and (100) faces, whereas nanoparticles and polycrystalline samples preferentially expose the (111) face, with small exposure of the (100) face. Catalytic studies show that the interaction of CO with ceria rods is substantially stronger than with nanoparticles, with a greater conversion rate for CO to CO_2 at a given temperature.[4] In ref 5, it was demonstrated that as ceria polycrystallites are aged and heated, (111) faces disappear, whereas (100) faces are now exposed. These aged samples have a greater activity for CO oxidation than the untreated samples, and this is concluded to be due to the presence of the more reactive (100) faces in the sample.

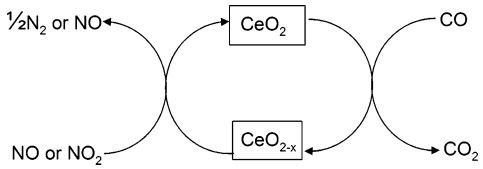

Figure 1. Schematic of the catalytic cycle involving oxidation of CO to CO_2 with concomitant reduction of the ceria surface.

This sensitivity of CO oxidation to the nature of the Miller index of the sample has been rationalized by considering the stabilities of the crystal faces exposed in the different ceria samples. It is by now well understood that the (111) surface is the most stable, followed by the (110) and (100) surfaces.[6,7] The ease of reduction of the surface was considered to follow the stability of the surfaces and it was concluded that the exposure of the less stable (= more reactive) (110) and (100) faces provided more reactive sites for interaction with the CO molecule and oxidation of CO to CO_2. [4,5,8]

Using interatomic potentials (IP), Sayle et al.[6] was able to compute the energy gained upon oxidation of CO with bulk ceria and the (111) and (110) surfaces, showing that on a surface,

* To whom correspondence should be addressed. E-mail: watsong@tcd.ie.
† School of Chemistry.
‡ Present address: Tyndall National Institute, Lee Maltings, Prospect Row, Cork, Ireland.
§ Trinity Centre for High Performance Computing.

10.1021/jp062499a CCC: $33.50
Published on Web 07/29/2006

the reaction is exothermic and most favorable on the (110) surface. Recently, Sayle et al.[8] has extended this work to a nanoparticle and found the reactivity of the nanoparticle to lie between the least reactive (111) surface and the more reactive (110) surface. However, more detailed atomic and electronic insights into the origin of the surface sensitivity to CO oxidation by ceria requires a quantum mechanical treatment.

Recently, Yang et al. published a density functional theory (DFT) study of the interaction between CO and the (111) and (110) surfaces of ceria[9] in which surface sensitivity to CO oxidation was studied. Weak physisorption is present on the (111) surface and strong and weak adsorption modes were found on the (110) surface, with formation of a (CO_3) species. However, because experiment shows that the surface is reduced and we and others have demonstrated that due to the presence of the self-interaction error DFT is not a suitable method for the study of reduced ceria,[7,10,11] the findings of ref 9 need to be revisited, e.g., the resulting atomic and electronic structure as well as the energetics involved. We have further demonstrated that an approach that corrects for the self-interaction error such as DFT+U (DFT corrected for on-site Coulomb interactions) needs to be employed to correctly describe reduced ceria surfaces.[7,11,12]

In the present work, we consider the DFT+U description of the interaction between CO and the (111), (110), and (100) surfaces of ceria, which is the first ab initio study in which the stoichiometric and reduced ceria surfaces involved in this important catalytic reaction are consistently described. We study in a consistent theoretical fashion for the first time the surface sensitivity of the adsorption structures, the electronic structure, and the energetics and derive an atomic level understanding of the surface sensitivity observed in experimental characterization of this reaction. These results allow us to understand in great detail the interactions driving the initial stages of surface reduction and CO oxidation.

2. Methods

The calculations presented herein were performed using the VASP code,[13] in which the valence electronic states are expanded in a basis of plane waves, whereas the strongly oscillating core electron wave functions are represented using the projector augmented wave (PAW) approach.[14] For our calculations, PAW can be considered as an all-electron approach with a frozen core to describe the core−valence interaction; we use a [He] core for oxygen and carbon and a [Xe] core for cerium. The Perdew−Wang 1991 generalized gradient approximation (GGA) for the exchange-correlation functional[15] is applied. For the DFT+U calculations, we have discussed the sensitivity of the results to the value of U,[7,11] and a value of 5 eV is used for all calculations in which Ce ions are present.

For three-dimensional (3-D) periodic boundary conditions, a surface is represented by a slab, which is separated from its images in the direction perpendicular to the surface by a vacuum gap; in this work, a vacuum gap of 15 Å is used. For the (111) surface, a slab 10.5 Å (12 atomic layers) thick is used; for the (110) surface the slab thickness is 11.5 Å (7 atomic layers), whereas for the (100) surface, a slab thickness of 10.94 Å (9 atomic layers) is applied. In all cases, a $p(2 \times 2)$ expansion of the surface unit cell is applied to reduce the defect−defect interactions present in periodic supercell calculations, giving a minimum distance of 7.65 Å between periodic images of the CO molecule (on the (100) surface). The cutoff energy for the plane wave basis is 500 eV and for sampling the Brillouin zone we use a $2 \times 2 \times 1$ Monkhorst Pack grid; sampling along the vector separating the slabs is not required. For the interaction of CO with the stoichiometric surface, we adsorb CO onto both sides of the slab in order that any dipole will be quenched. Full relaxation of the atomic positions of all adsorption structures is allowed and all calculations are spin polarized.

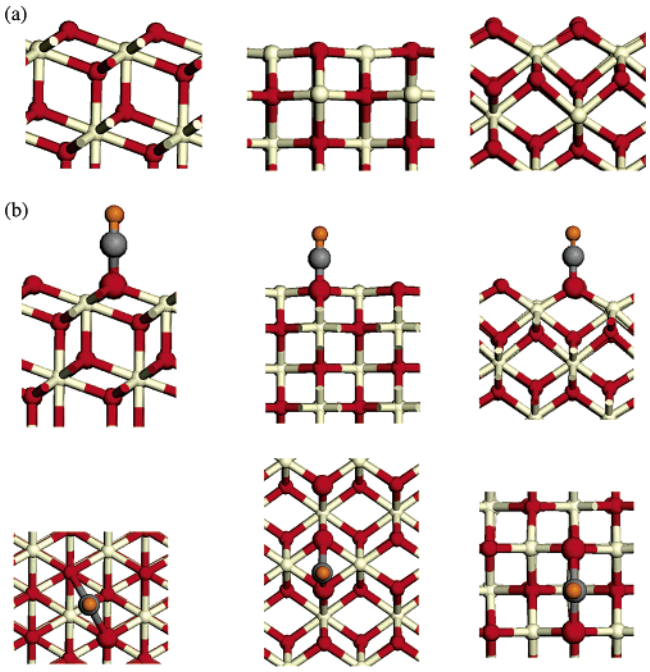

Figure 2. (a) Stoichiometric (111), (110), and (100) ceria surfaces. (b) Starting structures for CO adsorbed in a bridging configuration on the (111), (110), and (100) surfaces. The white spheres are Ce, the red spheres oxygen, the gray spheres carbon, and the orange spheres the oxygen of the CO molecule.

3. Results

We have considered adsorption of CO on the (111), (110), and (100) surfaces of ceria with a number of different configurations, which we now discuss. On each surface, the CO molecule can adsorb through the carbon atom onto a single surface cerium (Ce_s) or oxygen (O_s) atom, Figure 2. We consider only the interaction between the carbon atom of CO and O_s, because this should be the favorable interaction for CO_2 formation, in which an oxygen atom is pulled out of the lattice. Alternatively, the carbon atom can interact with two surface oxygen atoms (O_s), in which case the oxygen atoms are *bridged*, in a symmetric (where the carbon to O_s distances are equivalent) or an asymmetric configuration (with nonequivalent carbon to O_s distances).

For the case of the bridging adsorption mode, we consider one symmetric adsorption structure on the (111) and (110) surfaces, with a number of different possible initial adsorption structures on the (100) surface. Figure 2b shows the symmetric bridging modes on the surfaces. On the (100) surface, we further consider structures in which the CO molecule has moved off the line bridging the two surface oxygen atoms, as well as a structure in which the carbon atom is coordinated to 4 surface oxygen atoms and a "twisted" structure derived from the bridging structure in Figure 2b, through displacement of the surface oxygen atom atoms closest to the carbon atom

For the asymmetric bonding modes, we consider two possible modes on each surface. In both adsorption modes, there are two inequivalent C−O_s distances; in one configuration, the CO is displaced toward one of the oxygens, creating two inequivalent C−O_s distances, whereas in the other configuration, the CO is

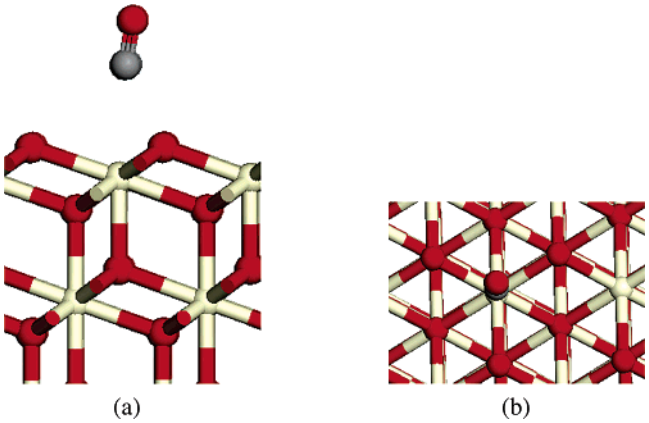

Figure 3. Relaxed geometry for CO on the (111) surface irrespective of the initial interaction. (a) side view, (b) plan view.

displaced toward one oxygen and off the line joining the two surface oxygen atoms.

To assess which structures require a more detailed analysis, we consider initially the adsorption energy for CO on a ceria surface, which is computed from

$$E_{ads} = E(CeO_2 - (CO)_{ads}) - [E(CeO_2) + E(CO)] \quad (1)$$

where $(CeO_2 - (CO)_{ads})$ is the structure resulting from adsorption of CO on the surface (we postpone discussion of the nature of this structure until later). Negative adsorption energies signify that the adsorption structure is stabilized compared to the initially isolated species. Small adsorption energies (on the order of less than 20 kcal/mol) signify a weak interaction between the molecule and the surface, and are usually coupled with little perturbation to either molecular or surface structure. Large adsorption energies (on the order of 20 kcal/mol or greater) signify a strong interaction between the molecule and the surface, which should be coupled with a strong perturbation to the structure of the molecule and the surface.

3.1. CO Adsorption on the (111) Ceria Surface. On the (111) surface, we find that, irrespective of the initial adsorption mode, the resulting surface−adsorbate structure is the same, with a weak interaction, resulting in an adsorption energy of −6 kcal/mol. The carbon atom lies 2.88 Å above a surface Ce atom, with distances to the three nearest surface oxygen atoms at 2.77, 3.49, and 3.05 Å. The resulting structure is presented in Figure 3 and shows an intact CO molecule that interacts weakly with an intact, stoichiometric surface. The small adsorption energy is consistent with our computed exothermic reaction energy of −13 kcal/mol for conversion of CO to CO_2 over this surface.[16] The IR spectroscopy study of Li et al.[3] also found that this weak adsorption mode was stable on ceria powders.

Examination of the electronic structure shows little change compared to stoichiometric ceria and free CO, e.g., the gap state between the top of the valence band and the unoccupied Ce 4*f* band, characteristic of reduced ceria, is not present, whereas the partial C and O density of states are very similar to free CO, which provides good evidence that the molecular species is still CO. The surface geometry, the weak adsorption energy, and the electronic structure all point to an unperturbed CO and ceria surface, and no further investigation of this interaction was considered.

3.2. CO Adsorption on the (110) Surface. For the case where the CO molecule is initially directed at a surface atom, we find an intact CO molecule physisorbed on the (110) surface, similar to the physisorbed structure found for the (111) surface;

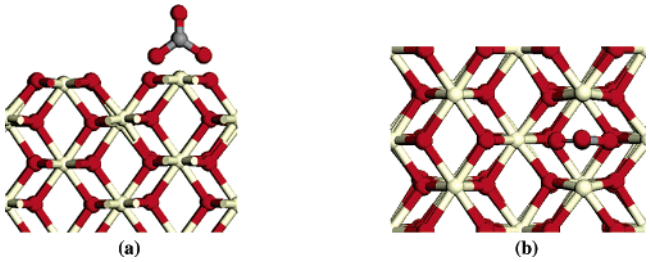

Figure 4. Relaxed structure of CO adsorbed on the (110) surface of ceria. (a) Front view, (b) plan view.

the adsorption energy is −5 kcal/mol for the physisorbed structure, with a distance from carbon to a surface Ce atom of 2.90 Å. Because a strongly chemisorbed bonding mode was also found, this bonding mode was not considered further.

In Figure 4, the fully relaxed structure for the initially symmetric bridging configuration of CO on the (110) ceria surface is shown. We calculate the adsorption energy to be −45 kcal/mol, indicating a strongly bound CO molecule on the surface. No initially asymmetric configuration is stable on this surface, and these all relax to either the strongly bound symmetric structure or to the physisorbed structure discussed above. The computed energy gain for the conversion of CO to CO_2 over this surface is −27 kcal/mol[16] consistent with the adsorption energy above.

In the symmetric bridging configuration on the (110) surface, two oxygen atoms are pulled out of the surface layer and a surface bound species with the appearance of a CO_3 group is formed (Figure 4a). In the CO_3 moiety, there is one C−O distance of 1.23 Å (derived from the interacting CO molecule), whereas the remaining two C−O distances are 1.37 Å. For comparison, we consider carbon−oxygen distances in other structures; in free CO: 1.14 Å (this work), in CO_2: 1.16 Å,[17] in $Ca(CO_3)$: 1.28 Å,[17] and in CH_3OH: 1.42 Å.[17] The C−O distances in the surface bound CO_3 on the (110) surface are more consistent with the C−O distances in carbonate, rather than in the other structures.

We consider now the effect of CO adsorption on the surface structure. CO adsorption pulls two oxygen atoms out of the surface layer, and the surface Ce ions bonded to these oxygen atoms are also displaced out of the surface layer. The distance between these Ce atoms is now 4.08 Å (3.89 Å in the pure surface). The remaining in-plane surface Ce−O distances contract to 2.30−2.31 Å. The contraction of the surface Ce−O distances is consistent with the geometry found for the bare reduced (110) surface.[11]

The surface Ce to subsurface oxygen distances are 2.36−2.38 Å, which is a lengthening of 0.14 Å compared to the pure surface. This arises due to the subsurface oxygen atoms moving off their lattice sites and out of the subsurface layer. This surface structure is consistent with that found in DFT+U calculations on a reduced (110) surface in which one oxygen atom was removed to form the vacancy.[11]

However, a complete assignment of the nature of the surface and the surface bound species requires an analysis of the electronic structure. In Figure 5, we show the Ce derived partial atomic and angular momentum decomposed EDOS (PEDOS). The DFT+U derived Ce PEDOS shows the same features as the electronic structure of the reduced (110) surface presented in our previous work.[11] In particular, the Ce PEDOS displays the presence of an occupied gap state (region II of Figure 5) between the top of the valence band (region I) and the empty Ce 4*f* manifold (region III). Previous experimental and theoretical studies of reduced ceria surfaces[7,10,11,19] show that the gap

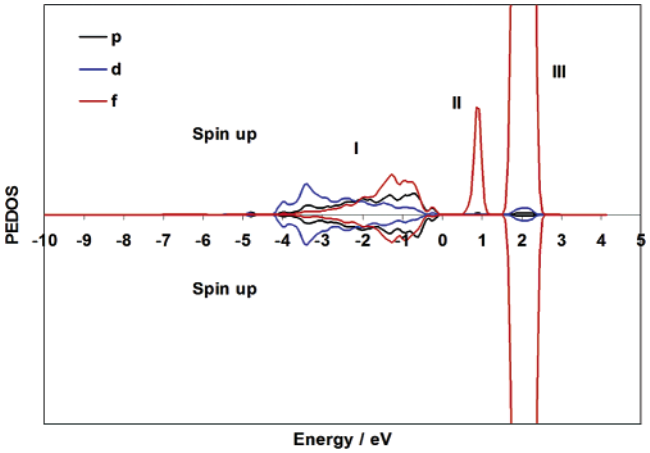

Figure 5. Cerium PEDOS for CO adsorbed on the (110) surface. The zero of energy is set to the energy of the state at the top of the valence band.

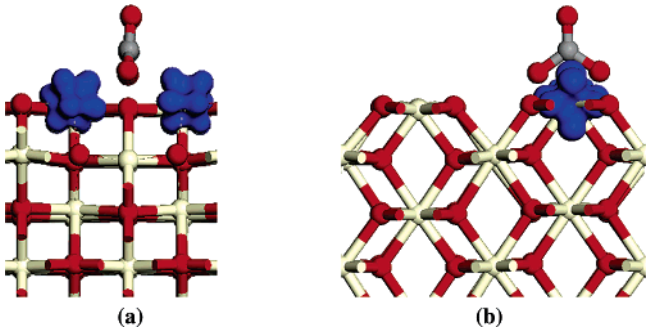

Figure 6. Spin density for CO adsorbed with a bridging configuration on the (110) ceria surface. (a) Side view, (b) front view.

state is due to partial occupation of Ce 4*f* states localized on the Ce atoms neighboring the site of an oxygen vacancy, which only appears upon reduction of a ceria surface. This indicates that the surface has been reduced due to interaction with the CO molecule; integration of the gap state yields 4 electrons, consistent with two Ce^{3+} on each surface of the slab. The energy gap from the O 2p valence band to this state is 1.00 eV, consistent with a calculated energy gap for the bare reduced surface of 1.20 eV.[11]

To further confirm the nature of the surface, the resulting excess spin density (defined as the difference between the up spin density and the down spin density) is displayed in Figure 6. Localization of spin is found on the two surface Ce ions that were previously bound to the two oxygen atoms extracted from the surface to form the CO_3 species. Consistent with the Ce PEDOS and the integrated Ce PEDOS, these Ce atoms have therefore been reduced to Ce(III) and the reduced surface remains insulating, completely consistent with the known behavior of reduced ceria surfaces.[7,11,19]

The C 2p and O 2p PEDOS from the 3 oxygen atoms and 1 carbon atom of the (CO_3) adsorbate structure is shown in Figure 7a. The zero of energy is set to the highest occupied molecular orbital (HOMO) of the adsorbate. O 2p derived states from the adsorbate are found at the top of the occupied states. Between −5 and −6 eV below the top of the valence band, we find two C 2p and O 2p derived states.

To establish the nature of the adsorbed surface species, we consider the possible chemical moieties that can be formed. First, the geometry of the adsorbed species is consistent with the geometry of the carbonate ion, $(CO_3)^{2-}$, and for comparison, we present the C and O 2p PEDOS from gas phase $(CO_3)^{2-}$ in

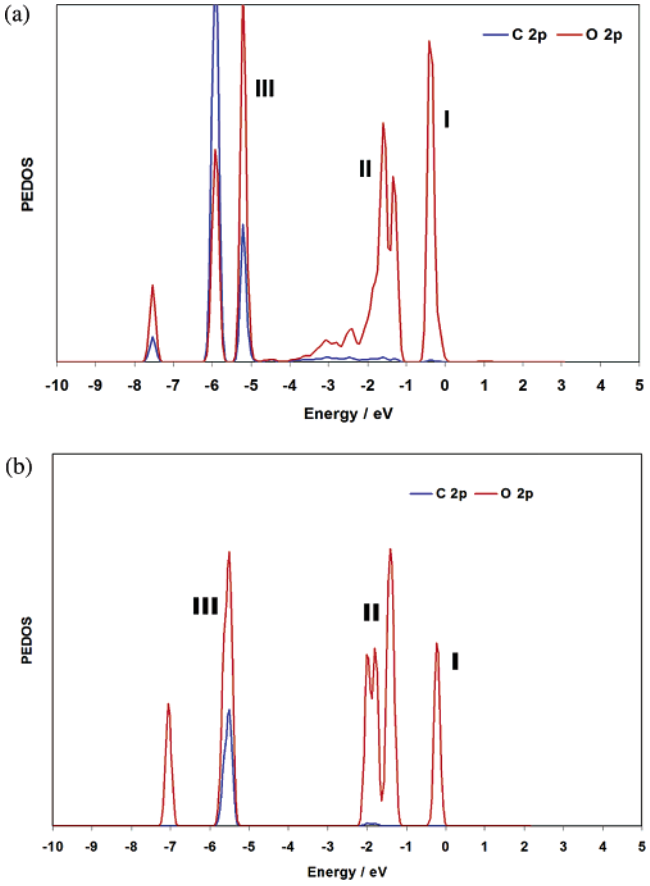

Figure 7. Oxygen and carbon 2p PEDOS from the 4 atoms in (a): adsorbed $(CO_3)^{2-}$ and (b): from gas phase $(CO_3)^{2-}$. The zero of energy is set to the energy of the state at the top of the occupied states in (a).

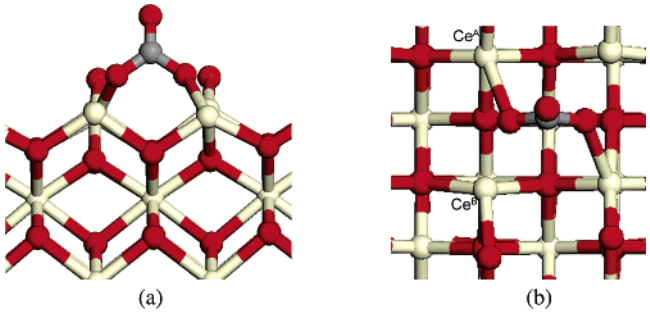

Figure 8. Relaxed surface structure for CO adsorbed on the (100) surface of ceria. (a) Side view, (b) plan view. In (b), Ce^A and Ce^B are marked (see text).

Figure 7b. In both cases, spin pairing characteristic of a closed shell system is present while the nature of the PEDOS peaks are very similar. The highest occupied state in the adsorbate and the carbonate ion (HOMO, region I in Figure 7) is an O 2p state. For carbonate, a second O 2p band (region II of Figure 9b), is found between −1 and −2 eV below the HOMO, with further C 2p and O 2p derived bands also present, region III of Figure 7b. Calculation of the integrated density of states for the carbon and oxygen atoms which make up the CO_3 group gives 23.7 electrons, compared to the 24 electrons expected for a carbonate $(CO_3)^{2-}$ group. This provides good evidence that an adsorbed carbonate group is present at the surface. Interaction of the CO molecule with lattice oxygen atoms pushes some O 2p derived states of region II down in energy, where interaction with the C 2p/O 2p states of region III now is possible, giving the adsorbate PEDOS in Figure 7a.

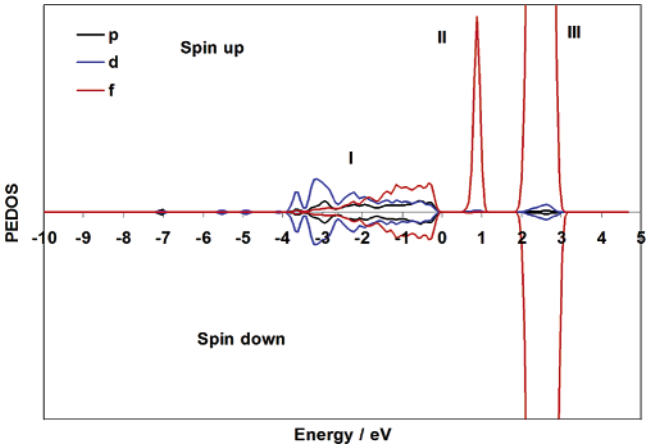

Figure 9. Ce PEDOS for CO adsorbed on the (100) surface.

Finally, the electronic structure of the adsorbed species also rules out the possibility of the adsorption structure being due to CO. The HOMO of the CO molecule is derived from O 2p and C 2p contributions, whereas the HOMO in Figure 7a is derived completely from O 2p states, with no C 2p contribution, ruling out CO as a possible adsorption species. Simple charge partitioning obtained from projection of the density of states onto spherical harmonics centered on the atomic sites, results in a transfer of 1.70 electrons to the adsorbed species, which further points to the adsorption structure of CO on the (110) ceria surface being carbonate, $(CO_3)^{2-}$.

3.3. CO Adsorption on the (100) Ceria Surface. In Figure 8, we show the relaxed structure for the initial symmetric bridging mode of CO on the (100) surface. The adsorption energies of the fully relaxed structures are −74 kcal/mol for the symmetric configuration. The computed energy gain for the conversion of CO to CO_2 is −20 kcal/mol (exothermic),[16] consistent with the strong adsorption energy. Of the other possible symmetric bonding modes for CO adsorption on this surface, the resulting relaxed structures are either a physisorbed configuration, with a positive adsorption energy or the symmetric bridging mode of Figure 8. The initial asymmetric bonding modes also relax to the symmetric structure of Figure 8.

We observe formation of a CO_3 group on the surface, similar to the adsorption structure on the (110) surface, whereby two surface oxygen atoms have been displaced by 0.65 Å from their initial lattice sites toward the carbon atom of the CO group. The two C−O distances involving these oxygen atoms are 1.37 Å, whereas the remaining C−O distance, derived from the CO molecule, is 1.21 Å. Although the geometry of the adsorbed moiety is not ideal for a carbonate ion, it is more consistent with a carbonate species than the other possible species.

The displacement of the surface oxygen atoms to form the CO_3 moiety leaves two elongated Ce−O distances for each of the two displaced oxygen atoms, with one Ce−O distance of 2.48 Å (which is denoted Ce^A in Figure 8b) and the other Ce−O distance being 2.52 Å (Ce^B in Figure 8b), an elongation of 0.29/0.33 Å compared to the pure surface. We also see that the Ce^B atoms are displaced away from their initial lattice sites in the pure surface, which lengthens the Ce^B−O bonds, as seen in Figure 8b. The Ce−O distances in the remainder of the surface reflect the modifications induced by CO adsorption. Ce^A and Ce^B are bonded to one further surface oxygen atom, with the Ce−O distances being 2.04 (Ce^A) and 2.31 Å (Ce^B). Similar to the (110) surface, a notable perturbation to the surface structure is observed upon adsorption of CO.

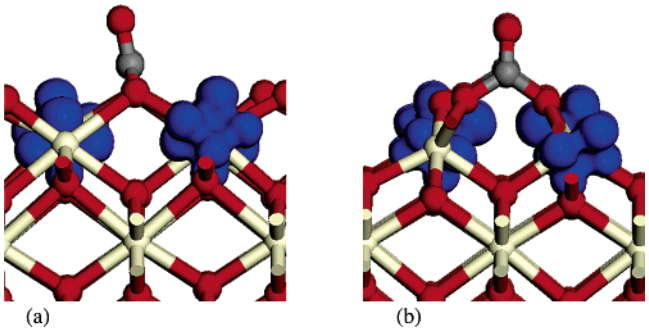

Figure 10. Spin density for CO on the (100) ceria surface. (a) Front view, (b) side view.

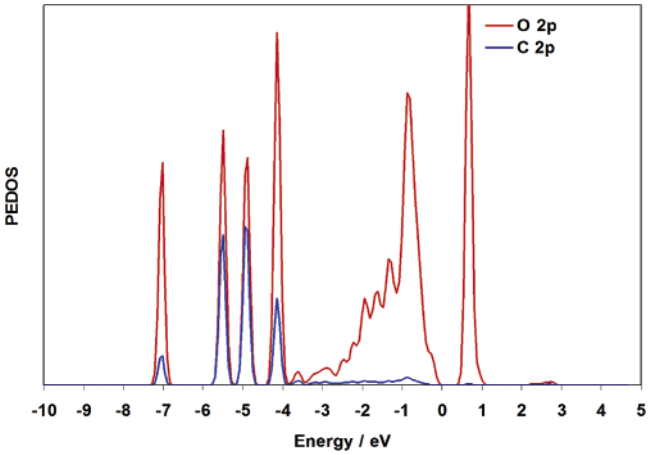

Figure 11. C 2p/O 2p PEDOS for the 4 atoms making up adsorbed (CO_3).

The Ce PEDOS in Figure 9 shows a Ce 4f derived gap state between the valence band and the unoccupied Ce 4f states (region II in Figure 9). Integration of this peak results in 4 electrons, that is, two electrons per surface in the simulation cell, confirming formation of Ce^{3+}. The energy gap between the top of the valence band and this state is 0.90 eV, which is consistent with that observed for the bare partially reduced surface.[6] The excess spin density is presented in Figure 10 and confirms the presence of charge localized on two surface Ce ions (the Ce^B ions). This demonstrates that the Ce^B ions are reduced to Ce (III), with a larger ionic radius than Ce(IV), with the elongated Ce−O distances a result of the larger ionic radius.

The surface bound species would appear to be a carbonate, and this would be consistent with the formation of Ce(III) ions, similar to the (110) surface. To establish the nature of the surface bound species, we again consider comparison of the C 2p/O 2p PEDOS of the 4 atoms in the adsorbed (CO_3) species (Figure 11) and the gas-phase carbonate ion (Figure 7b) to determine the nature of the adsorbate. In the PEDOS of adsorbed (CO_3), we find electronic states similar to those for the interaction with the (110) surface along with similar modifications to the lower energy (CO_3) derived states. We conclude that the surface bound species on the (100) surface is indeed closer in nature to $(CO_3)^{2-}$ rather than CO. As discussed for the (110) surface, the fact that the adsorbed species is $(CO_3)^{2-}$ means that only two Ce ions can be reduced to Ce(III), which is observed in the spin density in Figure 12. Thus, charge transfer from the surface to the CO molecule has occurred. Integrating the density of states for the adsorbed CO_3 group, we find 23.8 electrons, again consistent with a carbonate adsorbate on the surface.

4. Discussion

Our calculations show a strong surface dependence for the interaction of CO with ceria surfaces. For the (111) surface, we find a weak interaction, whereas for the (110) and (100) surfaces, we find a strong, but surface dependent, interaction. The origin of the surface dependence can be understood by considering the surface structure. A strong interaction between the surface and the CO molecule results in the formation of a carbonate species. This requires two surface oxygen atoms to be displaced from their lattice sites so as to interact with the carbon atom of the CO molecule, thus introducing a notable distortion of the surface. In the carbonate ion, the two surface oxygen atoms should ideally be 2.20 Å apart.

Because the formation of the carbonate species requires two oxygen atoms to be displaced from their lattice sites, this process is most favored if the oxygen atoms show low coordination, a short O−O distance in the surface, and can be easily pulled out of the surface. In the (111) surface, the oxygen atoms are 3 coordinate, whereas the O−O distance in the surface layer is 3.87 Å. In addition, the oxygen vacancy formation energy in the (111) surface is by far the largest of the three surfaces.[11,18] Taken together, these factors mean that distortion of the surface, in terms of displacing oxygen atoms from their surface sites, is difficult. In fact, no distortion to the surface is observed upon interaction with CO.

The distance between two surface oxygen atoms in the (110) surface is notably shorter, at 2.74 Å, with 3 coordinate surface oxygen atoms. The shorter O−O distance means that, despite the surface oxygen atoms being three coordinate, upon interaction with the CO molecule, it will cost less energy for two surface oxygen atoms to be pulled toward the carbon of CO, so that the carbonate structure can be formed; the two surface oxygen atoms are displaced inward toward the carbon atoms by 0.25 Å. This surface also has the lowest vacancy formation energy, indicating that the oxygen atoms will be more easily displaced on this surface compared with the (111) or (100) surfaces.

For the (100) surface, the displacement of the two surface oxygen atoms upon interaction with CO is 0.65 Å, yet the C−O distances in the surface bound (CO_3) are not as close to the carbonate geometry as they are in the (110) surface. The O−O distance in the pure (100) surface is 3.71 Å, which is larger than in the (110) surface and similar to the (111) surface. However, for this surface, the oxygen atoms are two coordinate and it also has a relatively low vacancy formation energy,[16] allowing considerable movement of oxygen atoms off their lattice sites. The large initial spacing of the oxygen atoms, however, would require a very large displacement of approximately 0.90 Å of the oxygen atoms to form an ideal $(CO_3)^{2-}$ structure, which is not seen. We can therefore conclude that the surface sensitivity for CO adsorption is a compromise between the energy required to displace the oxygen atoms off their lattice sites and the energy gained through formation of $(CO_3)^{2-}$. The different surface geometries thus lead to this surface sensitivity, with the (111) surface showing physisorption and the (110) and (100) surfaces showing chemisorption and surface reduction.

The electronic structure of the reduced surfaces derived from DFT+U is very different to that derived from GGA-DFT in ref 9. Although both approaches show a reduction of the ceria surface, the GGA-DFT results are inconsistent with the body of available data in the literature for reduced ceria surfaces, both experimental and computational. Most importantly, the gap state that is found in experimental studies[19] and DFT+U studies of reduced ceria[7,10,11] is not present in the results of ref 9. So far as we are aware, the delocalization of charge found in ref 9 has no basis in experimental findings, whereas the electronic structure of the reduced surfaces found in the present work is consistent with experimental data on reduced ceria, so that surface reduction leads to oxidation of CO to $(CO_3)^{2-}$.

Upon comparison with the available experimental data, we find that formation of a carbonate group on the (110) and (100) surfaces is consistent with the findings of refs 3−5. Li et al.[3] also found a configuration in which the carbon atom of CO points at the surface and the CO molecule remains intact, similar to the weak adsorption mode found on the (111) and (110) surfaces. Recent experimental data on polycrystalline ceria, nanoparticles, and nanorods, which expose different crystallographic faces, are also consistent with the present results. For polycrystalline ceria and nanoparticles, (111) faces are exposed and the reactivity of CO on these structures was found to be significantly less than on nanorods, which expose (110) and (100) faces. Activation of the CO molecule by electron transfer and formation of carbonate structures on the (110) and (100) surfaces and the lack of carbonate formation on the (111) surface along with a consideration of the stabilities of the reduced surfaces[11] provides a comprehensive explanation of the experimental results found in refs 4 and 5.

Conclusions

To contribute to the understanding of the mechanism of CO oxidation over ceria surfaces, we have considered the interaction of CO with stoichiometric ceria surfaces using the DFT+U approach. On the (111) surface, interaction with the CO molecule leads to weak adsorption, with an adsorption energy of −6 kcal/mol. For the (110) and (100) surfaces, interaction with CO leads to formation of a surface $(CO_3)^{2-}$ species, in which two oxygen atoms are pulled out of the surface. The interaction has an adsorption energy of −45 kcal/mol (110) and −74 kcal/mol (100), consistent with the exothermic reaction energies for formation of CO_2. The formation of surface-bound carbonate-like structures on the (110) and (100) surfaces and the accompanying surface distortions are consistent with the findings of refs 4 and 5, in which CO was found to be reactive only on exposed (110) or (100) faces of nanoparticles and nanorods of ceria, rather than on exposed (111) faces.

Analysis of the electronic structure for the (110) and (100) surfaces shows formation of the Ce 4*f* derived gap state between the valence band and the unoccupied Ce 4*f* states, which is a characteristic signature of reduced ceria. The excess spin density and the partial charge density analysis of this state confirms that these Ce 4*f* states are localized on two Ce^{3+} ions at the surface. Further analysis of the geometry and electronic structure confirms the presence of a carbonate ion $(CO_3)^{2-}$ at the surface, in agreement with experimental data. Thus, with strong chemisorption of CO on a stoichiometric ceria surface, the molecule is oxidized and the ceria surface is reduced.

We have demonstrated that the DFT+U approach can provide a description of the adsorption of molecules on ceria surfaces, which is consistent with experimental findings and thus advances our understanding of the processes involved in ceria-based catalysis.

Acknowledgment. We acknowledge support for this work from the donors of the Petroleum Research Fund administered by the American Chemical Society and Science Foundation Ireland (Grant Number 04/BR/C0216). We also acknowledge the EPSRC for funding of and access to the Mott2 computer at

Rutherford Appleton Laboratory, under Grant GR/S84415/01, and the IITAC project for funding of and access to the TCHPC computational facilities through a PRTLI cycle III grant.

References and Notes

(1) Trovarelli, A. *Catalysis by Ceria and Related Materials*; Imperial College Press: London, UK, **2002**.

(2) Bedrane, S.; Descorme, C.; Duprez, D. *Catal. Today*, **2002**, *75*, 401; Li, W.; Gracia, F. J.; Wolf, E. E. *Catal. Today*, **2003**, *81*, 437; Tang, X.; Zhang, B.; Li, Y.; Xu, Y.; Xin, Q.; Shen, W. *Catal. Today*, **2004**, *93*−*95*, 183.

(3) Li, C.; Sakata, Y.; Arai, T.; Domen, K.; Maruya, K.; Onishi, T. *J. Chem. Soc. Faraday Trans. 1* **1989**, *85*, 929; Li, C.; Sakata, Y.; Arai, T.; Domen, K.; Maruya, K.; Onishi, T. *J. Chem. Soc. Faraday Trans. 1* **1989**, *85*, 1451.

(4) Zhou, K.; Wang, X.; Sun, X.; Ping Q.; Li, Y. *J. Catal*. **2005**, *229*, 206.

(5) Aneggi, E.; Llorca, J.; Boaro, M.; Trovarelli, A. *J. Catal*. **2005**, *234*, 88.

(6) Sayle, T. X. T.; Parker, S. C.; Catlow, C. R. A. *Chem. Commun*. **1992**, 977.

(7) Nolan, M.; Grigoleit, S.; Sayle, D. C.; Parker, S. C.; Watson, G. W. *Surf. Sci*. **2005**, *576*, 217.

(8) Sayle, T. X. T.; Parker, S. C.; Sayle, D. C. *Phys. Chem. Chem. Phys*. **2005**, *7*, 2936.

(9) Yang, X. Z.; Woo, T. K.; Hermansson, K. *Chem. Phys. Lett*. **2005**, *396*, 384.

(10) Fabris, S.; Vicario, G.; Balducci, G.; de Gironcoli, S.; Baroni, S. *J. Phys. Chem. B* **2005**, *109*, 22860; Kresse, G.; Blaha, P.; Da Silva, J. L. F.; Ganduglia-Pirovano, M. V. *Phys. Rev. B: Condens. Matter Mater. Phys.* **2005**, *72*, 237101; Fabris, S.; de Gironcoli, S.; Baroni, S.; Vicario, G.; Balducci, G. *Phys. Rev. B: Condens. Matter Mater. Phys.* **2005**, *72*, 237102.

(11) Nolan, M.; Parker, S. C.; Watson, G. W. *Surf. Sci.* **2005**, *595*, 223.

(12) Anisimov, V. I.; Zaanen, J.; Andersen, O. K., *Phys. Rev B: Condens. Matter Mater. Phys.* **1991**, 44, 943; Dudarev, S. L.; Botton, G. A.; Savrasov, S. Y.; Humphreys, C. J.; Sutton, A. P. *Phys. Rev. B: Condens. Matter Mater. Phys.* **1998**, *57*, 1505.

(13) Kresse, G.; Hafner, J. *Phys. Rev. B: Condens. Matter Mater. Phys.* **1994**, *49*, 14251; Kresse, G.; Furthmüller, J. *Comput. Mater. Sci*. **1996**, *6*, 15.

(14) Blöchel, P. E. *Phys. Rev. B: Condens. Matter Mater. Phys.* **1994**, *50*, 17953; Joubert, D.; Kresse, G. *Phys. Rev. B: Condens. Matter Mater. Phys.* **1999**, *59*, 1758.

(15) Perdew, J. P. In *Electron Structure of Solids*; Ziesche, P., Eschrig H., Eds.; Akademie Verlag: Berlin, 1991.

(16) Nolan, M.; Parker, S. C.; Watson, G. W. *Phys. Chem. Chem. Phys*. **2006**, *8*, 216.

(17) CO_2: Thomas, J. R.; DeLeeuw, B. J.; Vacek, G.; Crawford, T. D.; Yamaguchi, Y.; Schaefer, H. F. *J. Chem. Phys.* **1993**, *99*, 403; Graner, G.; Rossetti, C.; Baily, D. *Mol. Phys*. **1986**, *58*, 627. Ca(CO_3): Maslen, E. N.; Streltsov, V. A.; Streltsova, N. R. *Acta. Cryst*. **1993**, *B49*, 636; Skinner, A. J.; LaFemina, J. P.; Jansen, H. J. F. *Am. Mineral*. **1994**, *79*, 205. CH_3OH: Miani, A.; Hänninen, V.; Horn, M.; Halonen, L. *Mol. Phys*. **2000**, *98*, 1737.

(18) Yang, X. Z.; Woo, T. K.; Hermansson, K. *J. Chem. Phys*. **2004**, *120*, 7741.

(19) Henderson, M. A.; Perkins, C. L.; Engelhard, M. H.; Thevuthasan, S.; Peden, C. H. F. *Surf. Sci*. **2003**, *526*, 1.